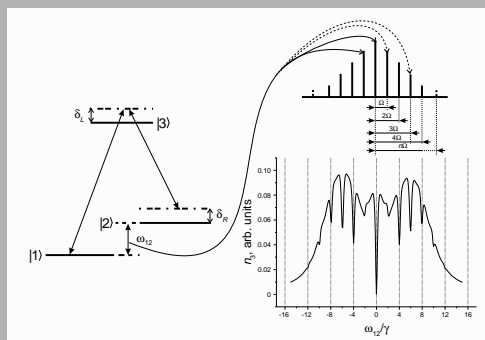


**Abstract:** Dynamics of a three-level quantum system in  $\Lambda$ -configuration driven by a resonant laser field with and without frequency modulation (FM) is studied for the first time in detail using two simulation techniques – the density matrix and quantum trajectories analysis. This analysis was applied to the FM-spectroscopy of coherent dark resonances in Cs atoms and computer simulation results for the absorption spectra are in qualitative agreement with those taken in an experiment.



Mechanism of forming the dark resonances for the case of the  $\Lambda$ -system interacting with the frequency-modulated laser field

© 2006 by Astro Ltd.  
Published exclusively by WILEY-VCH Verlag GmbH & Co. KGaA

## Computer modeling of frequency-modulation spectra of coherent dark resonances

J. Vladimirova,<sup>1</sup> B. Grishanin,<sup>1</sup> V. Zadkov,<sup>1,\*</sup> V. Biancalana,<sup>2</sup> G. Bevilacqua,<sup>2</sup> Y. Dancheva,<sup>2</sup> and L. Moi<sup>2</sup>

<sup>1</sup> International Laser Center and Faculty of Physics, M.V. Lomonosov Moscow State University, Moscow 199899, Russia

<sup>2</sup> Department of Physics, University of Siena, via Roma 56, 53100 Siena, Italy

Received: 15 May 2006, Accepted: 20 May 2006

Published online: XX XXXXXXXX 2006

**Key words:** coherent dark resonances; frequency-modulation spectroscopy

**PACS:** 42.50.Gy, 32.70.Jz, 32.10.Dk

### 1. Introduction

The coherent population trapping (CPT) phenomenon is currently widely used in different applications such as magnetometry, metrology, and others [1–6]. It is most conspicuous for the  $\Lambda$ -system formed of two closely spaced long lived levels optically coupled to a third distant short lived level by two continuous coherent radiation fields (Fig. 1). In absorption spectra, coherent superposition of the closely spaced levels leads to a very narrow dip of induced transparency or, equivalently, to a non-absorbing dark resonance when the resonance fluorescence is observed.

The basics of CPT phenomenon are well understood in the frame of three-level analytical model [7]. For the case of multilevel systems, however, such simple model has to be significantly complicated and analytical results in most cases became impossible [8]. Enriched energetic structure

of multilevel atoms, especially in the presence of an external magnetic field, also results in essential modification of the resonance dependencies on the parameters of the fields driving the system.

Despite the conventional experimental technique for observing the dark resonances spectra with the use of two resonant laser fields described above is now widely used for many applications, still there is a need in elaborating simpler experimental techniques, which would, for instance, employ only one laser field, but with frequency modulation (FM), that also allow spectroscopy of the coherent dark resonances in multilevel atoms. Such experiments are conducted by the group of Prof. L. Moi at the University of Siena in Italy [9] and they, in fact, initiated the current theoretical study of interaction between the three-level system in  $\Lambda$ -configuration with the frequency-modulated laser field.

\* Corresponding author: e-mail: zadkov@phys.msu.ru

In a typical experiment on FM-spectroscopy of coherent dark resonances of Cs atoms, the atomic media is placed in a homogeneous magnetic field, which value is in the range of few 10  $\mu$ T. The coherent resonance is observed when the laser emission, which is frequency modulated, contains in its spectrum frequency components that are in resonance with the atomic levels, i.e., the frequency difference between these components matches the Zeeman splitting  $\omega_{12}$  of the ground-state sublevels (Fig. 1) due to the presence of dc magnetic field. The laser spectrum is tailored via diode laser frequency modulation obtained by direct modulation of the laser junction current. The coherent structure can be then seen scanning the modulation frequency in a small range around the two-photon resonance condition, or at a fixed modulation frequency scanning the magnetic field in the corresponding range [9–12].

Despite obvious simplicity of this method and numerous applications of FM-techniques in microwave, NMR, and optical spectroscopy [13], analysis of the spectrum becomes a separate problem as a theoretical model for the FM-spectroscopy of dark resonances does not exist to our knowledge so far<sup>1</sup>.

In this paper, we present a detailed study of the dynamics of a three-level quantum system in  $\Lambda$ -configuration driven by resonant laser field with and without frequency modulation using two computer simulation techniques – the density matrix and quantum trajectories analysis. Our studies show that analytical consideration of the problem is impossible in this case.

The paper is organized as follows. General theoretical background for both density matrix and quantum trajectories analysis used for numerical simulation of the fluorescence and absorption spectra of the driven  $\Lambda$ -system is given in Sec. 2. In Sec. 3 two considered above computer simulation techniques are applied for the analysis of a driven  $\Lambda$ -system in both cases, when the frequency modulation is switched off (Sec. 3.1) and on (Sec. 3.2), respectively. Calculations are made for the absorption intensity. Finally, the conclusions are summarized in Sec. 4.

## 2. Theoretical analysis of temporal dynamics of a driven $\Lambda$ -system

In experiments on FM-spectroscopy of coherent dark resonances, the total absorption/transmission of the  $\Lambda$ -system is measured. The total absorption in case when the relaxation processes in the system are only due to the decay of the upper state is equal to the losses thanks to the fluorescence. Total intensity of the spontaneous fluorescence

<sup>1</sup> It is worth to note that interaction of a two-level system with FM-field has been studied in detail, even in analytical form [13]. Further generalization of the theory onto the case of multilevel systems, three-level systems specifically, does not exist to our knowledge so far.

is proportional to the stationary value of the excited state population:

$$I_{fl} \sim \langle \hat{n}_3 \rangle = \text{Tr} \hat{n}_3 \hat{\rho}. \quad (1)$$

Therefore, calculation of the total absorption of the  $\Lambda$ -system is reduced to the calculation of the excited state population  $n_3$ .

In this section, we will focus on the numerical simulation techniques, which can be adequately used for simulating fluorescence/absorption spectrum of both a model  $\Lambda$ -system and a multilevel atom driven by the FM laser field(s). With these notes in mind, there exist two key computer simulation techniques suitable for our purpose, namely, the technique based on the solving the master equations for the density matrix (we will call it the *density matrix analysis*) and quantum trajectories technique (we will call it the *quantum trajectories analysis*) [14–17].

In application to the analysis of multilevel atomic systems, the key difference between these two techniques is outlined below. The density matrix technique is used primarily for analysis of atomic systems with rather limited number  $N$  of energy levels because the number  $N^2$  of master equations describing the system can become too large for real multilevel atoms (like Cs or Rb) and, therefore, such analysis would require relevant computer resources. By contrast, the quantum trajectories analysis of the multilevel atomic system with large number  $N$  of energy levels requires computational resources proportional to  $N$  and, therefore, has an advantage here. Despite this difference, each of the two techniques has its own advantages and drawbacks, so that we intentionally consider both of them to clarify which one is better and in which situation.

### 2.1. Density matrix analysis

We will start with the density matrix analysis, when the dynamics of a quantum system is described with the density matrix time dependence of which is defined by the following kinetic, i.e., *master equation*:

$$\dot{\hat{\rho}} = -\frac{i}{\hbar} [\hat{H}, \hat{\rho}] + \mathcal{L}_r \hat{\rho}, \quad (2)$$

where first term in the right part of the equation describes reversible dynamics of the system with the hamiltonian  $\hat{H}$  and second term – nonreversible contribution to the dynamics due to the stochastic interaction of the system with the reservoir, which is described with the relaxation superoperator  $\mathcal{L}_r$ . In assumption that interaction of the system with the reservoir can be described with a diffusion type process, the relaxation superoperator can be represented by the secondary commutator with the hamiltonian  $\hat{H}_\xi$  of the system-reservoir interaction, averaged over the reservoir noise  $\hat{\xi}(t)$ .

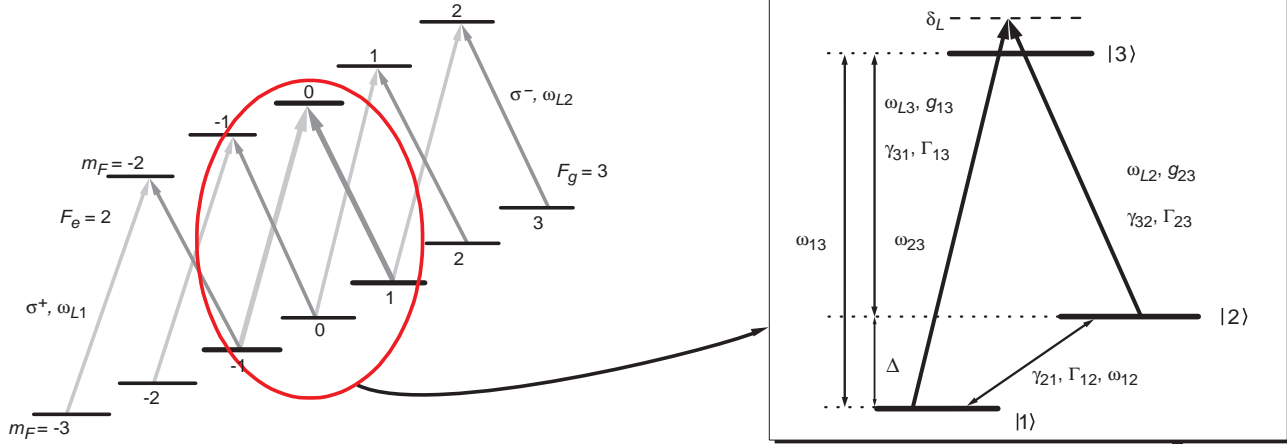


**Figure 1** (online color at www.lphys.org)  $\Lambda$  systems formed of the Zeeman sublevels in the  $F_g = 3 \rightarrow F_e = 2$  transitions excited by the  $\sigma^+$  and  $\sigma^-$  components of the respective frequencies  $\omega_1$  and  $\omega_2$ , whose difference is equal to the splitting of the Zeeman sublevels with  $\Delta m_F = 2$ . Three-level system in  $\Lambda$ -configuration has the following parameters:  $\omega_{L1}$ ,  $\omega_{L2}$  are the frequencies of the laser fields driving transitions of the system;  $\Omega_{13}$ ,  $\Omega_{23}$  are the respective Rabi frequencies;  $\delta_L$  is the frequency detuning from the  $|1\rangle \leftrightarrow |3\rangle$  transition;  $\gamma_{31}$ ,  $\gamma_{32}$  are the decay rates from excited state  $|3\rangle$  onto the low-lying levels  $|1\rangle$  and  $|2\rangle$ ;  $\gamma_{12}$  and  $w$  are the decay and pumping rates of the level  $|1\rangle$  via the level  $|2\rangle$ , correspondingly;  $\Gamma_{31}$ ,  $\Gamma_{32}$ , and  $\Gamma_{12}$  are the dephasing rates for the transitions  $|1\rangle \leftrightarrow |3\rangle$ ,  $|2\rangle \leftrightarrow |3\rangle$ , and  $|1\rangle \leftrightarrow |2\rangle$ , respectively

Then, the relaxation term  $\mathcal{L}_r \rho$  in master equation (2) can be written in the general Lindblad form [18] as

$$\mathcal{L}_r = -\frac{1}{2} \sum_m (\hat{C}_m^+ \hat{C}_m \odot + \odot \hat{C}_m^+ \hat{C}_m) + \sum_m \hat{C}_m \odot \hat{C}_m^+, \quad (3)$$

where  $\odot$  is the substitution symbol to be replaced with the density matrix  $\hat{\rho}$ , operators  $\hat{C}_m$  describe interaction with the reservoir, operators  $\hat{C}_m^+$  are conjugated to the operators  $\hat{C}_m$  and both of them have dimension  $(1/t)^{1/2}$ .

It is worth to note that representation (3) preserves interpretation of  $\hat{\rho}$  as the density matrix, i.e., the normalization condition  $\text{Tr} \hat{\rho} = 1$  and positivity of the probability  $\langle \psi | \hat{\rho} | \psi \rangle$  to find the system in any state  $|\psi\rangle$  are fulfilled at any time moment and for any initial states  $\hat{\rho}(t=0)$ . Note also that Eq. (3) does not require that  $\hat{C}_m$  must be defined uniquely when they are chosen phenomenologically to represent an a priori known relaxation process.

In the right side of Eq. (3) providing the total probability contribution  $(d/dt)\text{Tr} \hat{\rho} dt \equiv 0$  the first sum is the anti-commutator, which consists of the terms decreasing the total population  $\text{Tr} \hat{\rho}$ , as far as the second sum increases it. The number of operators  $\hat{C}_m$  in Eq. (3) in general case can be rather large because each operator corresponds to a specific decay channel. For the case of spontaneous emission in a two-level system, for instance, there exists only one operator because we consider only one decay channel, i.e., spontaneous decay. This operator has the form  $\hat{C}_1 = \Gamma^{1/2} \hat{\sigma}^-$ , where  $\hat{\sigma}^- = |g\rangle\langle e|$  is the atomic transition operator from the ground state  $|g\rangle$  onto the excited state  $|e\rangle$ . More examples are described in [17].

For the case of a  $\Lambda$ -system, in order to write the operators  $\hat{C}_m$  one has to take into account the following relaxation processes: spontaneous decay from the excited state  $|3\rangle$ , incoherent decay and incoherent pumping of the two ground levels  $|1\rangle$ ,  $|2\rangle$ . Operator  $\hat{C}_m$  in this case will consist of four terms responsible for the above listed relaxation processes, namely, operators  $\hat{C}_1$  and  $\hat{C}_2$  describe spontaneous decay from the excited state  $|3\rangle$  onto the ground states  $|1\rangle$ ,  $|2\rangle$ , operators  $\hat{C}_3$  and  $\hat{C}_4$  describe incoherent decay and incoherent pumping of the level  $|1\rangle$  to the level  $|2\rangle$ :

$$\begin{aligned} \hat{C}_1 &= (\gamma_{31})^{1/2} \hat{P}_{13}, & C_1^+ &= (\gamma_{31})^{1/2} \hat{P}_{31}, \\ \hat{C}_2 &= (\gamma_{32})^{1/2} \hat{P}_{23}, & C_2^+ &= (\gamma_{32})^{1/2} \hat{P}_{32}, \\ \hat{C}_3 &= (\gamma_{21})^{1/2} \hat{P}_{12}, & C_3^+ &= (\gamma_{21})^{1/2} \hat{P}_{21}, \\ \hat{C}_4 &= (\mu_{12})^{1/2} \hat{P}_{21}, & C_4^+ &= (\mu_{12})^{1/2} \hat{P}_{12}, \end{aligned} \quad (4)$$

where  $\hat{P}_{kl}$  are the transition operators, which are represented, in general case, by the matrices with the only non-zero  $kl$ -element  $\hat{P}_{kl}(k, l) = 1$ .

With the help of Eqs. (3), (4) the relaxation term  $\mathcal{L}_r \hat{\rho}$  in master equation (2) takes the form:

$$\begin{pmatrix} \alpha_1 & \alpha_2 & \alpha_3 \\ \alpha_4 & \alpha_5 & \alpha_6 \\ \alpha_7 & \alpha_8 & \alpha_9 \end{pmatrix}, \quad (5)$$

where  $\alpha_1 = -\mu_{12}\rho_{11}(t) + \gamma_{21}\rho_{22}(t) + \gamma_{31}\rho_{33}(t)$ ,  $\alpha_2 = -0.5(\gamma_{21} + \mu_{12})\rho_{12}(t)$ ,  $\alpha_3 = -0.5(\gamma_{31} + \gamma_{32} + \mu_{12})\rho_{13}(t)$ ,

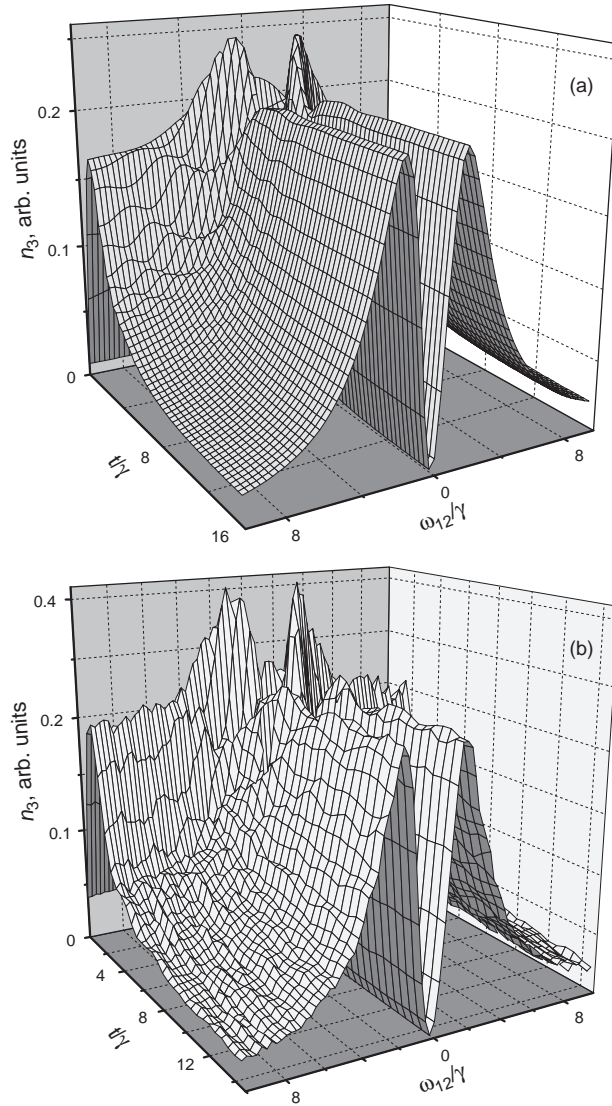


**Figure 2** Temporal dependence of the excited state population from a driven  $\Lambda$ -system calculated with the help of density matrix approach (a) and using quantum trajectories technique (b). Both plots show similar dependence of the excited state population  $n_3$  versus time since the excitation of the system and the ground state frequency splitting  $\omega_{12}$ . For simplicity, the calculations were made for the case of a symmetric  $\Lambda$ -system, i.e., for the equal Rabi frequencies  $\Omega_{13} = \Omega_{23} = 1$  and equal spontaneous decay rates  $\gamma_{31} = \gamma_{32} = \gamma = 1$  from the excited state; relaxation parameters of the ground state were set to zero. The number of computed quantum trajectories for figure (b) is equal to 2000

$\alpha_4 = -0.5(\gamma_{21} + \mu_{12})\rho_{12}(t)$ ,  $\alpha_5 = \mu_{12}\rho_{11}(t) - \gamma_{21}\rho_{22}(t) + \gamma_{32}\rho_{33}(t)$ ,  $\alpha_6 = -0.5(\gamma_{31} + \gamma_{32} + \gamma_{21})\rho_{23}(t)$ ,  $\alpha_7 = -0.5(\gamma_{31} + \gamma_{32} + \mu_{12})\rho_{13}(t)$ ,  $\alpha_8 = -0.5(\gamma_{31} + \gamma_{32} + \gamma_{21})\rho_{23}(t)$ ,  $\alpha_9 = -(\gamma_{31} + \gamma_{32})\rho_{33}(t)$ , and  $\gamma_{31}$ ,  $\gamma_{32}$  are the spontaneous decay rates,  $\gamma_{12}$  and  $\mu_{12}$  are the de-

cay and pumping rates of the level  $|1\rangle$  via the level  $|2\rangle$ , respectively.

Now, master equation (2) can be integrated numerically for a given Hamiltonian  $\hat{H}$  of the system and then all its necessary characteristics can be modeled.

## 2.2. Quantum trajectories analysis

Another relevant approach to model the temporal behavior of a  $\Lambda$ -system is the quantum trajectories analysis [14–17], which uses, instead of the time-dependent density matrix, a properly defined statistically-equivalent stochastic temporal dynamics of the wave function with the following averaging of the results by analogy with the Monte-Carlo method.

Modeling evolution of the wave function on the discretization interval  $dt$ , which ensures identical results with the solution of the master equation (2), includes two parts: i) modeling continuous variation of the current state and ii) modeling quantum jumps occurring randomly with certain probability.

Let us assume that the system at time  $t$  is in the state  $|\psi(t)\rangle$ . Then, the continuous variation of the current state can be described with the temporal dynamics of the wave function  $|\psi^{(1)}(t)\rangle$ , which is governed by the Schrödinger equation

$$|\psi^{(1)}(t + \delta t)\rangle \approx \left(1 + \frac{1}{i\hbar}\hat{H}dt\right)|\psi(t)\rangle \quad (6)$$

with the non-hermitian hamiltonian

$$\hat{H} = \hat{H} - \frac{i\hbar}{2} \sum_m \hat{C}_m^+ \hat{C}_m. \quad (7)$$

New wave-function is not normalized because the hamiltonian  $\hat{H}$  is a non-hermitian one and the squared norm of the function is equal to  $\langle\psi^{(1)}(t + dt)|\psi(t + dt)\rangle = 1 - \delta p$ , where  $\delta p$  has the form:

$$\delta p = \sum_m \delta p_m = dt \sum_m \langle\psi(t)|\hat{C}_m^+ \hat{C}_m|\psi(t)\rangle, \quad (8)$$

where the time step  $dt$  must fulfill the inequality  $\delta p \ll 1$ .

Random behavior of the wave function is described with the probability  $\delta p$  of quantum jumps. If the quantum jump does not occur with the probability  $1 - \delta p$ , the wave function  $|\psi^{(1)}(t + \delta t)\rangle$  must be renormalized to unit and then it will be mapped with the corresponding normalized function  $|\psi(t + \delta t)\rangle$ . When the quantum jump occurs, the wave-function transfers into the state  $\hat{C}_m|\psi(t)\rangle$  with the related probability  $\delta p_m/\delta p$ . Thus, at the time moment  $t + \delta t$  we do have one of the two normalized wave-functions:

- with the probability  $1 - \delta p$  the quantum jump does not occur and  $|\psi(t + \delta t)\rangle = |\psi^{(1)}(t + \delta t)\rangle(1 - \delta p)^{-1/2}$ ,
- with the probability  $\delta p_m$  the quantum jump occurs and  $|\psi(t + \delta t)\rangle = \hat{C}_m|\psi(t)\rangle(\delta p_m/\delta t)^{-1/2}$ .

### 3. Modeling absorption of a driven $\Lambda$ -system

#### 3.1. Case when the frequency modulation is switched off

Before studying interaction of a  $\Lambda$ -system with the FM laser field, let us first analyze a simpler problem – how the  $\Lambda$ -system interacts with a resonant laser field without frequency modulation.

##### 3.1.1. Density matrix analysis

Let us consider a three-level quantum system in  $\Lambda$ -configuration, which interacts with the field  $E(t) = E_0 \cos(\omega_0 t + \varphi)$ . In the basis of the atom energy states  $|1\rangle, |2\rangle, |3\rangle$  and at the choice of the unperturbed atomic motion in the form of the free precession of the  $|3\rangle$  state with the laser frequency  $\omega_0$  the interaction hamiltonian has the form:

$$\hat{H} = \frac{\hbar}{2} \begin{pmatrix} 0 & 0 & \Omega_{13} \\ 0 & -\omega_{12} & \Omega_{23} \\ \Omega_{13} & \Omega_{23} & \delta_L \end{pmatrix}, \quad (9)$$

where  $\Omega_{13}, \Omega_{23}$  are the Rabi frequencies,  $\delta_L = \omega_0 - \omega_{13}$  is the one-photon frequency detuning of the probe laser field, and  $\omega_{12}$  is the frequency shift between the two ground levels (see Fig. 1).

Substituting relaxation operator (3) in Eq. (2) we receive the following set of differential equations for essential density matrix elements:

$$\begin{aligned} \dot{\rho}_{11}(t) &= -\mu_{12}\rho_{11}(t) + \gamma_{21}\rho_{22}(t) + \gamma_{31}\rho_{33}(t) + \quad (10) \\ &+ i[\Omega_{13}\rho_{13}(t) - \Omega_{13}\rho_{31}(t)], \\ \dot{\rho}_{12}(t) &= -\Gamma_{12}\rho_{12}(t) - i[\omega_{12}\rho_{12}(t) + \Omega_{23}\rho_{13}(t) - \\ &- \Omega_{13}\rho_{32}(t)], \\ \dot{\rho}_{13}(t) &= -\Gamma_{13}\rho_{13}(t) + i[\Omega_{13}\rho_{11}(t) + \Omega_{23}\rho_{12}(t) + \\ &+ \delta_L\rho_{13}(t) - \Omega_{13}\rho_{33}(t)], \\ \dot{\rho}_{22}(t) &= \mu_{12}\rho_{11}(t) - \gamma_{21}\rho_{22}(t) + \gamma_{32}\rho_{33}(t) + \\ &+ i[\Omega_{23}\rho_{23}(t) - \Omega_{23}\rho_{32}(t)], \\ \dot{\rho}_{23}(t) &= -\Gamma_{32}\rho_{23}(t) + i[\Omega_{13}\rho_{21}(t) + \Omega_{23}\rho_{22}(t) + \\ &+ \omega_{12}\rho_{23}(t) + \delta_L\rho_{23}(t) - \Omega_{23}\rho_{33}(t)], \\ \dot{\rho}_{33}(t) &= i[-\Omega_{13}\rho_{13}(t) - \Omega_{23}\rho_{23}(t) + \Omega_{13}\rho_{31}(t) + \\ &+ \Omega_{23}\rho_{32}(t)] - (\gamma_{31} + \gamma_{32})\rho_{33}(t), \\ \dot{\rho}_{21}(t) &= \dot{\rho}_{12}^*(t), \quad \dot{\rho}_{31}(t) = \dot{\rho}_{13}^*(t), \quad \dot{\rho}_{32}(t) = \dot{\rho}_{23}^*(t). \end{aligned}$$

Integrating this set of differential equations we obtain a complete picture of temporal dynamics of the driven  $\Lambda$ -system and can calculate any its characteristic. As soon as we are interested in the total absorption of the  $\Lambda$ -system,

which is proportional to the excited state population, one needs simply to calculate the population (1) of the excited state  $|3\rangle$ . This temporal dependency is shown in Fig. 2a versus the frequency splitting  $\omega_{12}$  between two ground levels.

From Fig. 2 one can see that for the case when only one laser field with the frequency  $\omega_L$  acts on both transitions  $|1\rangle \leftrightarrow |2\rangle$  and  $|2\rangle \leftrightarrow |3\rangle$  of the  $\Lambda$ -system, the dark resonance is observed at  $\omega_{12} = \omega_L - \omega_L = 0$ , i.e., for the case of degenerate  $\Lambda$ -system. In experiment, such a resonance corresponds to the case when an external magnetic field is applied to produce the field depending frequency splitting of the ground state sublevels.

##### 3.1.2. Quantum trajectories analysis

We will consider only two actually essential radiation decay channels from excited state  $|3\rangle$  onto the low-lying states  $|1\rangle, |2\rangle$ , reducing the number of operators  $\hat{C}_m$  in Eq. (3) just to two operators:  $\hat{C}_1 = (\gamma_{31})^{1/2}\hat{P}_{13}$  and  $\hat{C}_2 = (\gamma_{32})^{1/2}\hat{P}_{23}$ .

Inserting  $\hat{C}_1$  and  $\hat{C}_2$  into Eq. (3), we obtain the following equation for the relaxation term:

$$\mathcal{L}_r \hat{\rho} = \begin{pmatrix} \gamma_{31}\rho_{33}(t) & 0 & -\Gamma\rho_{13}(t) \\ 0 & \gamma_{32}\rho_{33}(t) & -\Gamma\rho_{23}(t) \\ -\Gamma\rho_{13}(t) & -\Gamma\rho_{23}(t) & -2\Gamma\rho_{33}(t) \end{pmatrix}, \quad (11)$$

where  $\Gamma = (\gamma_{31} + \gamma_{32})/2$ . In accordance with the results of Sec. 2.2, the non-hermitian interaction hamiltonian is given by Eq. (7). Substituting  $\hat{C}_1$  and  $\hat{C}_2$  in this equation leads to the hamiltonian of the form:

$$\hat{H} = \frac{\hbar}{2} \begin{pmatrix} 0 & 0 & \Omega_{13} \\ 0 & -\omega_{12} & \Omega_{23} \\ \Omega_{13} & \Omega_{23} & -i\Gamma + \delta_L \end{pmatrix}, \quad (12)$$

where we assume that  $\gamma_{31} = \gamma_{32} = \gamma$ .

From the Schrödinger equation (6) one can readily obtain the following set of differential equations for the probability amplitudes  $a_1(t)$ ,  $a_2(t)$ , and  $a_3(t)$ :

$$\begin{aligned} \dot{a}_1(t) &= -i\Omega_{13}a_3(t), \quad (13) \\ \dot{a}_2(t) &= -i[-\omega_{12}a_2(t) + \Omega_{23}a_3(t)], \\ \dot{a}_3(t) &= -i[\Omega_{13}a_3(t) + \Omega_{23}a_2(t) + (-i\Gamma + \delta_L)a_3(t)]. \end{aligned}$$

Let us assume then that initially at  $t = 0$  all population in the system was equally distributed among the states  $|1\rangle$  and  $|2\rangle$ , i.e.,  $n_1 = n_2 = 1/2$ . Then, the set of equations (13) can be integrated using the quantum trajectories technique, which leads to the time-dependent wave-functions and, respectively, to the temporal dependencies of the population of the system's levels.

Temporal dependency of the excited state population calculated with the help of quantum trajectories technique is shown in Fig. 2b versus the frequency detuning  $\omega_{12}$  of the two ground states. From Fig. 2b one can clearly see

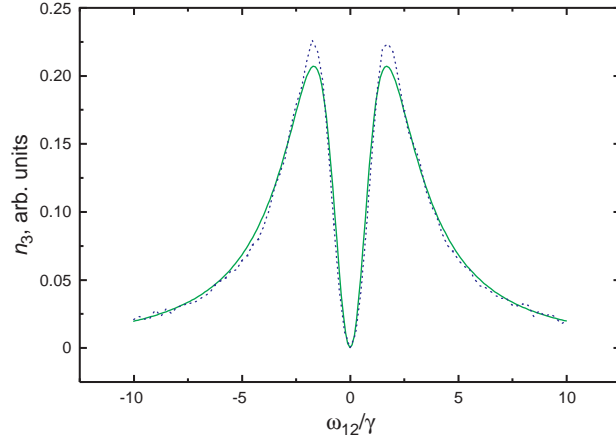


**Figure 3** (online color at [www.lphys.org](http://www.lphys.org)) Calculated population of the excited state of the symmetric  $A$ -system ( $\gamma_{31} = \gamma_{32} = \gamma$ ,  $\Gamma = 1$ ) versus  $\omega_{12}$  for  $\Omega_{13} = \Omega_{23} = 1$  received with the help of density matrix approach (solid line) and quantum trajectories technique (dotted line, the number of computed trajectories is equal to 2000) at  $t/\Gamma = 14$ , i.e., in the steady-state case

that the stationary solution is reached at the time of the order of  $10\gamma$ .

A more detailed comparison of the simulation results obtained by the density matrix approach and with quantum trajectories technique is shown in Fig. 3. It clearly shows that both methods give similar results and the curves are coincide rather well.

### 3.2. Case when the frequency modulation is switched on

In this Section, we will analyze the absorption spectrum of the  $A$ -system driven by a resonant frequency-modulated laser field  $E(t)$  with the carrier frequency  $\omega_0$ , which for the case of harmonic modulation with the modulation index  $M$  and frequency modulation  $\Omega$  can be written as

$$E(t) = E_0 \exp[i(\omega_0 t + M \sin \Omega t)] = \quad (14)$$

$$= E_0 \exp(i\omega_0 t) \sum_{n=-\infty}^{+\infty} J_n(M) \exp(in\Omega t).$$

In this series expansion, the Bessel functions  $J_n(M)$  characterize the frequency components of the frequency-modulated light, i.e., the amplitudes of the respective spectrum components are proportional to the Bessel functions for the fixed modulation index  $M$ . Fig. 4 shows how the spectrum changes with changing the modulation index  $M$  and the modulation frequency  $\Omega$ . When the modulation frequency  $\Omega$  is fixed, increasing the modulation index leads to the increasing the number of bands in the spectrum with the interbands distance being equal to  $\Omega$ .

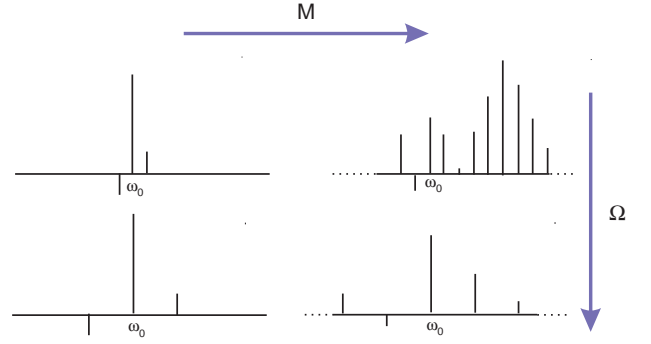


**Figure 4** (online color at [www.lphys.org](http://www.lphys.org)) Modification of the spectrum of the the frequency-modulated laser field due to the variations in the modulation frequency  $\Omega$  and the modulation index  $M$ . Increasing the modulation index  $M$  enlarges the number of sidebands in the spectrum, whereas increasing the modulation frequency  $\Omega$  enlarges the frequency separation between the sidebands

#### 3.2.1. Density matrix analysis

The interaction hamiltonian of the  $A$ -system interacting with the frequency-modulated laser field  $E(t) = E_0 \exp[i(\omega_0 t + M \cos \Omega t)] + c.c.$  has the form:

$$\hat{H} = \begin{pmatrix} 0 & 0 & e^{i\Delta(t)} \Omega_{13} \\ 0 & -\omega_{12} & e^{i\Delta(t)} \Omega_{23} \\ e^{-i\Delta(t)} \Omega_{13} & e^{-i\Delta(t)} \Omega_{23} & \delta_L \end{pmatrix}, \quad (15)$$

where  $\Delta(t) = M \sin \Omega t$ . Inserting equation for  $\mathcal{L}_r(\rho_S)$  in the form (5) into Eq. (2), we obtain the following set of differential equations:

$$\begin{aligned} \dot{\rho}_{11}(t) &= -\mu_{12}\rho_{11}(t) + \gamma_{21}\rho_{22}(t) + \gamma_{31}\rho_{33}(t) + \quad (16) \\ &+ i[e^{-i\Delta(t)} \Omega_{13}\rho_{13}(t) - e^{i\Delta(t)} \Omega_{13}\rho_{31}(t)], \\ \dot{\rho}_{12}(t) &= -\Gamma_{12}\rho_{12}(t) + i[-\omega_{12}\rho_{12}(t) + \\ &+ e^{-i\Delta(t)} \Omega_{23}\rho_{13}(t) - e^{-i\Delta(t)} \Omega_{13}\rho_{32}(t)], \\ \dot{\rho}_{13}(t) &= -\Gamma_{13}\rho_{13}(t) + i[e^{i\Delta(t)} \Omega_{13}\rho_{11}(t) + \delta_L\rho_{13}(t) + \\ &+ e^{i\Delta(t)} \Omega_{23}\rho_{12}(t) - e^{i\Delta(t)} \Omega_{13}\rho_{33}(t)], \\ \dot{\rho}_{22}(t) &= \mu_{12}\rho_{11}(t) - \gamma_{21}\rho_{22}(t) + i[e^{-i\Delta(t)} \Omega_{23}\rho_{23}(t) - \\ &- e^{i\Delta(t)} \Omega_{23}\rho_{32}(t)] + \gamma_{32}\rho_{33}(t), \\ \dot{\rho}'_{23}(t) &= -\Gamma_{23}\rho_{23}(t) + i[\Omega_{13}\rho_{21}(t) + e^{i\Delta(t)} \Omega_{23}\rho_{22}(t) + \\ &+ \delta_L\rho_{23}(t) + \omega_{12}\rho_{23}(t) + e^{i\Delta(t)} \Omega_{23}\rho_{33}(t)], \\ \dot{\rho}_{33}(t) &= i[-e^{-i\Delta(t)} \Omega_{13}\rho_{13}(t) - e^{-i\Delta(t)} \Omega_{23}\rho_{23}(t) + \\ &+ e^{i\Delta(t)} \Omega_{13}\rho_{31}(t) + e^{i\Delta(t)} \Omega_{23}\rho_{32}(t)] - \\ &-(\gamma_{31} + \gamma_{32})\rho_{33}(t), \end{aligned}$$

$$\dot{\rho}_{21}(t) = \dot{\rho}_{12}^*(t), \quad \dot{\rho}_{31}(t) = \dot{\rho}_{13}^*(t), \quad \dot{\rho}_{32}(t) = \dot{\rho}_{23}^*(t).$$

Solving this set of equations by analogy with Sec. 3.1.1, one can calculate the temporal dependence of the populations of the  $\Lambda$ -system levels.

The temporal dynamics of forming the spectrum of the dark resonance at the fixed modulation frequency and for two values of the modulation index is shown in Fig. 5. Simple analysis of this dynamics shows that with increasing the modulation index the structure of the spectrum is enriched and the number of sideband resonances is increased, too.

Qualitatively, the mechanism of forming the additional dark resonances in the spectrum of a  $\Lambda$ -system under the action of a frequency-modulated laser field is clarified in Fig. 6. Every time a narrow dark resonance is formed when the frequency splitting  $\omega_{12}$  between two ground levels of the  $\Lambda$ -system exactly matches the frequency difference between two neighboring sidebands in the spectrum of the incident frequency-modulated laser field. All pairs of the components of the incident laser field spectrum with the frequency shift between them equal to the modulation frequency  $\Omega$  (for instance, the pair marked by the solid line with arrows in Fig. 6) contribute to the dark resonance for which  $\omega_{12} = \Omega$ . Also, all the pairs of the components of the incident laser field spectrum frequency shift between which is equal to the doubled modulation frequency  $2\Omega$  (for example, the pair marked with the dashed lines with arrows in Fig. 6) contribute to the dark resonance for which  $\omega_{12} = 2\Omega$  and so on. From this consideration it follows that the frequency shift between the neighboring resonances in the observed spectrum of the  $\Lambda$ -system is equal to the modulation frequency  $\Omega$ .

The resulting rather complicated spectrum of the  $\Lambda$ -system irradiated with the FM resonant laser field is shown in Fig. 7, which plots the population of the excited state of the  $\Lambda$ -system versus the  $\omega_{12}$  frequency at the fixed modulation frequency  $\Omega = 2$  for various values of the modulation index. At  $M = 0$ , we have no modulation at all and the dark resonance is observed at  $\omega_{12} = 0$ , i.e., we have the case of degenerated  $\Lambda$ -system. Increasing further the modulation index leads to appearing of additional resonances in the spectrum at the conditions  $\omega_{12} = n\Omega$ ,  $n = \pm 1, \pm 2, \pm 3, \dots$ . This is because the number of sidebands in the spectrum of the incident laser field increases with increasing the modulation index in accordance with Eq. (14).

Amplitudes of these sidebands in the spectrum of the incident FM laser field are proportional to the Bessel functions  $J_n(M)$  at the fixed value of the modulation index  $M$  and decreasing up to zero with increasing  $n$ . Therefore, the number of sidebands in the spectrum of the incident laser field in the central part of the spectrum is approximately equal to  $M$ . Respectively, the resulting spectrum of the  $\Lambda$ -system shows also approximately  $M$  dark resonances in the central part of the spectrum. Fig. 8 confirms this result.

One can clearly see that at  $M = 5$  (Fig. 8a) the resonance at the frequency  $\omega_{12} = \pm 2\Omega$  practically vanishes.

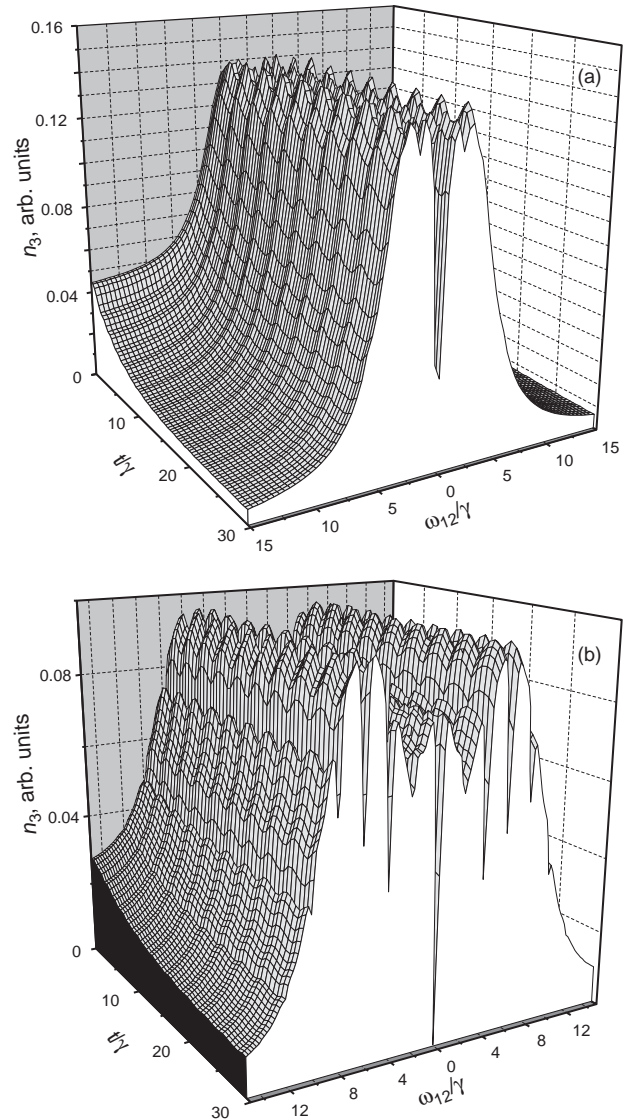


**Figure 5** Excited state population of the  $\Lambda$ -system versus time since the excitation of the system and  $\omega_{12}$  at the fixed modulation frequency  $\Omega = 2$  for two values of the modulation index  $M = 1.5$  (a) and  $M = 4$  (b). Other parameters were chosen as follows:  $\Omega_{13} = \Omega_{23} = 0.8$ ,  $\gamma_{31} = \gamma_{32} = 1$

At  $M = 10$  (Fig. 8b), the resonances at the frequencies  $\omega_{12} = \pm\Omega$ ,  $\pm 3\Omega$ , and  $\pm 6\Omega$  are vanished, as well. This happens because the two-photon dark resonances are observed on the background of the one-photon ones. As it has been shown in [19], for example, the power of the modulated signal transmitted through the media is proportional to the squared Bessel function  $J_n^2(M)$  for the given  $M$ . Keeping in mind that the Bessel function takes zero values at  $n = \pm 2$  for  $M = 5$  and at  $n = \pm 1, \pm 3, \pm 6$  for  $M = 10$ , this clarifies why the resonances at the frequencies  $n\Omega$  for these values of  $n$  are practically vanished.

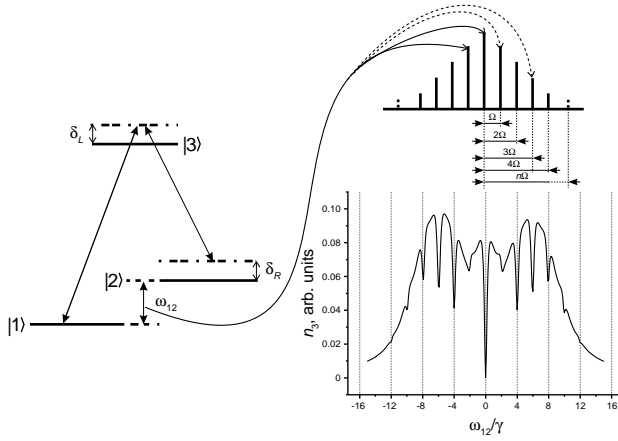


**Figure 6** Mechanism of forming the dark resonances for the case of the  $A$ -system interacting with the FM laser field

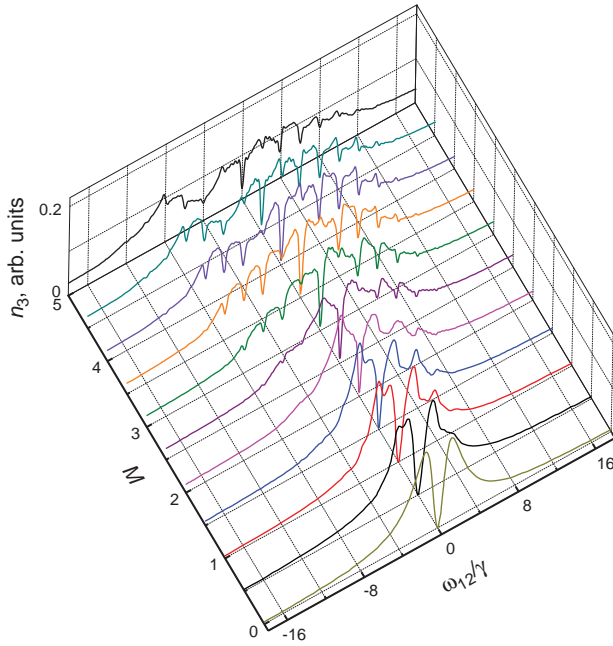


**Figure 7** (online color at [www.lphys.org](http://www.lphys.org)) Excited state population versus  $\omega_{12}$  and the modulation index  $M$ . Other parameters were chosen as follows:  $\Omega = 2$ ,  $\Omega_{13} = \Omega_{23} = 0.8$ ,  $\gamma_{31} = \gamma_{32} = \gamma = 1$

### 3.2.2. Quantum trajectories analysis

In accordance with the results of Sec. 2.2, the non-hermitian interaction hamiltonian of the  $A$ -system interacting with the frequency-modulated laser field  $E(t) = E_0 \exp[i(\omega_0 t + M \cos \Omega t)] + c.c.$  is given by Eq. (7). Sub-

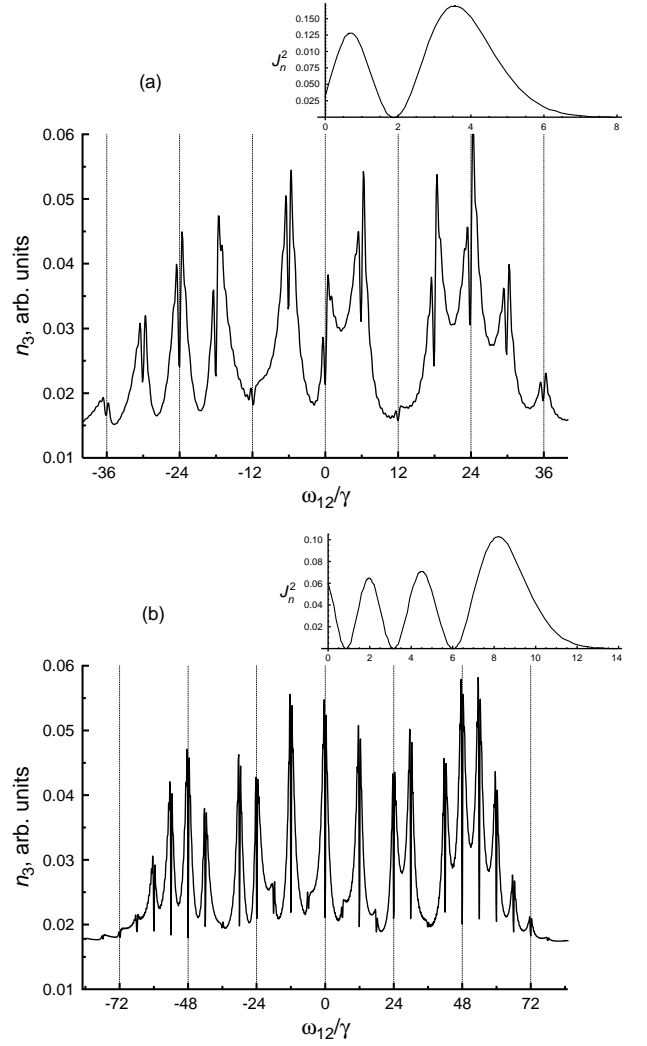


**Figure 8** Population of the excited state in the symmetric  $A$ -system versus  $\omega_{12}$  for two fixed values of the modulation index  $M = 5$  (a) and  $M = 10$  (b) at the modulation frequency  $\Omega = 6$  a.u. and the Rabi frequencies  $\Omega_3 = \Omega_{23} = 0.8$ . Insets show the respected squared Bessel functions  $J_n^2(M)$

stituting  $\hat{C}_1$  and  $\hat{C}_2$  (from Sec. 3.1.2) in this equation leads to the hamiltonian of the form:

$$\hat{H} = \begin{pmatrix} 0 & 0 & e^{i\Delta(t)}\Omega_{13} \\ 0 & -\omega_{12} & e^{i\Delta(t)}\Omega_{23} \\ e^{-i\Delta(t)}\Omega_{13} & e^{-i\Delta(t)}\Omega_{23} & \delta_L - i\Gamma \end{pmatrix}, \quad (17)$$

where

$$\Delta(t) = M \sin \Omega t, \quad \Gamma = \frac{\gamma_{31} + \gamma_{32}}{2}, \quad \gamma_{31} = \gamma_{32} = \gamma.$$

From the Schrödinger equation (6) one can readily obtain the following set of differential equations for the probability amplitudes  $a_1(t)$ ,  $a_2(t)$ , and  $a_3(t)$ :

$$\dot{a}_1(t) = -ie^{i\Delta(t)}\Omega_{13}a_3(t), \quad (18)$$

$$\begin{aligned}\dot{a}_2(t) &= -i[-\omega_{12}a_2(t) + e^{i\Delta(t)}\Omega_{23}a_3(t)], \\ \dot{a}_3(t) &= -i[e^{i\Delta(t)}\Omega_{13}a_3(t) + e^{i\Delta(t)}\Omega_{23}a_2(t) + \\ &+ (-i\Gamma + \delta_L)a_3(t)].\end{aligned}$$

Let us assume by analogy with Sec. 3.1.2 that at the initial time moment  $t = 0$  all population in the system is distributed in between two ground levels  $|1\rangle$  and  $|2\rangle$ , i.e.,  $n_1 = n_2 = 0.5$ . Then, solving set of equations (18) with the help of quantum trajectories technique we will receive time-dependent wave-functions of the system and time-dependent populations of each of the energetic levels.

Temporal dependency of the population of the excited state calculated with the help of quantum trajectories versus the frequency spacing between two ground levels  $\omega_{12}$  is shown in Fig. 9. The calculations were done for the same parameters as similar calculations by density matrix approach (Sec. 3.2.1). Comparison of both these methods is shown in Fig. 9b. One can easily see from this figure that results obtained by two different methods are in good agreement. Some quantitative difference is because the number of calculated trajectories is not an infinite one, but equal only to 5000. Increasing the number of trajectories in a computer experiment will lead to more precise coincidence of the results, but is timeconsuming. However, even our results show that the quantum trajectories technique can be adequately used for simulating not only three level system in  $\Lambda$ -configuration interacting with the frequency-modulated field, but also can be used for simulating more complicated multilevel systems.

## 4. Conclusions

In conclusion, we have presented a theoretical model for the FM-spectroscopy of the coherent dark resonances on example of a three-level quantum system in  $\Lambda$ -configuration driven by resonant laser field with and without frequency modulation using two simulation techniques – the density matrix and quantum trajectories analysis. With these techniques, such physical quantities as the total fluorescence intensity in equilibrium and in the transient response, resonance fluorescence spectrum, linear and nonlinear absorption coefficients, and the refractive indices, which can be all measured experimentally, can be modeled within the frame of the proposed model.

As an example, we calculated the total absorption for the real atomic  $\Lambda$ -system formed of the Zeeman sublevels of one of the two alkali hyperfine ground states in Cs atoms. The calculated spectrum using such a simplified model is in a qualitative agreement with the experimental results reported in the literature [9, 10] and it is clearly seen that at high laser modulation index additional side CPT-resonances are present. Their frequency positions matches the experimental ones and it can be seen that CPT resonance appear when  $n\Omega$  (where  $n$  is an integer number) equals the Zeeman splitting of two sublevels  $\omega_{12}$ .

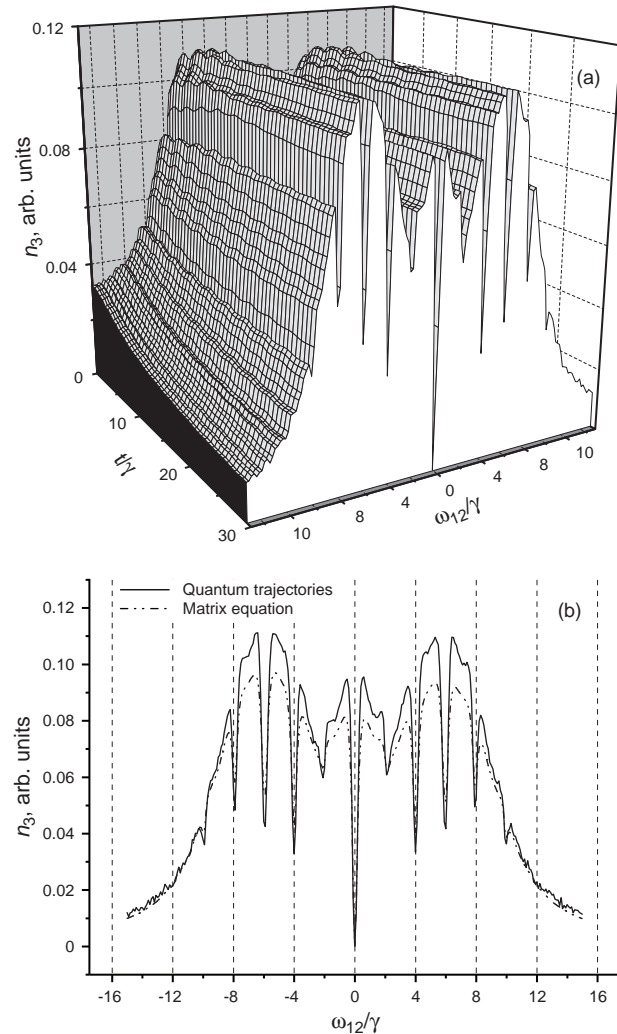


**Figure 9** a) Excited state population of the  $\Lambda$ -system versus time since the excitation of the system and  $\omega_{12}$  at the fixed modulation frequency  $\Omega = 2$  for the modulation index  $M = 4$ . Other parameters were chosen as follows:  $\Omega_{13} = \Omega_{23} = 0.8$ ,  $\Gamma = 1$ . b) Excited state population of the  $\Lambda$ -system versus  $\omega_{12}$  for the parameters of (a) computed with the help of density matrix approach (solid line) and quantum trajectories techniques (dashed line). The number of computed trajectories is equal to 1000

Our future work will be concentrated on elaboration of more complex model, where a larger number of experimental parameters will be considered. Moreover, we plan to extend the model by considering a richer level structure, which is well reasonable using the method of quantum trajectories analysis, whose computing time increases linearly with the number  $N$  of the considered levels, in contrast with the quadratic dependency shown by the density matrix approach.

*Acknowledgements* This work was partially supported by the Russian Foundation for Basic Research under the grant No. 04-02-17554.

## References

- [1] G. Alzetta, A. Gozzini, L. Moi, and G. Orriols, *Nuovo Cimento B* **36**, 5 (1976).
- [2] H.R. Gray, R.M. Whitly, and C.R. Stroud, Jr, *Opt. Lett.* **3**, 218 (1978).
- [3] G. Alzetta, L. Moi, and G. Orriols, *Nuovo Cimento B* **52**, 209 (1979).
- [4] G. Alzetta, L. Moi, and G. Orriols, *Opt. Commun.* **42**, 335 (1982).
- [5] A. Aspect, E. Arimondo, R. Kaiser, N. Vansteenkiste, and C. Cohen-Tannoudji, *Phys. Rev. Lett.* **61**, 826 (1996).
- [6] A. Kasapi, *Phys. Rev. Lett.* **77**, 3908 (1997).
- [7] E. Arimondo, in: E. Wolf (ed.), *Progress in Optics* (Elsevier, Amsterdam, 1996), **35**, p. 257.
- [8] Yu.V. Vladimirova, B.A. Grishanin, V.N. Zadkov, N.N. Kolachevskii, A.V. Akimov, N.A. Kisilev, and S.I. Kanorskii, *J. Theor. Exp. Phys.* **96**, 629 (2003).
- [9] C. Andreeva, G. Bevilacqua, V. Biancalana, S. Cartaleva, Y. Dancheva, T. Karaulanov, C. Marinelli, E. Mariotti, and L. Moi, *Appl. Phys. B* **76**, 667 (2003).
- [10] G. Bevilacqua, V. Biancalana, E. Breschi, Y. Dancheva, C. Marinelli, E. Mariotti, L. Moi, Ch. Andreeva, T. Karaulanov, S. Cartaleva, 13-th Int. School on Quantum Electr.: Laser Physics and Applications, *Proc. SPIE* **5830**, 150 (2005).
- [11] E.B. Alexandrov, M. Azuzinsh, D. Budker, D.F. Kimbal, S.M. Rochester, and V.V. Yashchuk, <http://arxiv.org>, *Physics* 0405049 (2004).
- [12] Yu. Malakyan, S.M. Rochester, D. Budker, D.F. Kimbal, and V.V. Yashchuk, *Phys. Rev. A* **69**, 013817 (2004).
- [13] G.E. Hall and S.W. North, *Annu. Rev. Phys. Chem.* **51**, 243 (2000).
- [14] J. Dalibard, Y. Castin, and K. Molmer, *Phys. Rev. Lett.* **68**, 5 (1992).
- [15] K. Mølmer and Y. Castin, *Quantum Semiclass. Opt.* **8**, 49 (1996).
- [16] H.J. Carmichael, *Phys. Rev. Lett.* **70**, 15 (1993).
- [17] K. Mølmer, Y. Castin, and J. Dalibard, *J. Opt. Soc. Am. B* **10**, 524 (1993).
- [18] G. Lindblad, *Commun. Math. Phys.* **48**, 119 (1976).
- [19] J.M. Supplee, E.A. Whittaker, and W. Lenth, *Appl. Opt.* **33**, 6294 (1994).